Di-Substituted Cyclohexyl Derivatives Bind to Two Identical Sites with Positive Cooperativity on the Voltage-Gated Potassium Channel, $K_v1.3$

William A. Schmalhofer,[‡,§] Robert S. Slaughter,[‡,§] Mary Matyskiela,[‡,§] John P. Felix,[‡] Yui S. Tang,[||] Kathleen Rupprecht,[⊥] Gregory J. Kaczorowski,[‡] and Maria L. Garcia*[,‡]

Departments of Ion Channels, Drug Metabolism, and Medicinal Chemistry, Merck Research Laboratories, P.O. Box 2000, Rahway, New Jersey 07065

Received January 21, 2003; Revised Manuscript Received March 6, 2003

ABSTRACT: Di-substituted cyclohexyl (DSC) derivatives inhibit the voltage-gated potassium channel, $K_v1.3$, and have immunosuppressant activity (Schmalhofer et al. (2002) *Biochemistry 41*, 7781−7794). This class of inhibitors displays Hill coefficients of near 2 in functional assays, and trans DSC analogues appear to selectively interact with $K_v1.3$ channel conformations related to C-type inactivation. To further understand the details of the DSC inhibitor interaction with potassium channels, *trans*-1-(*N*-*n*-propylcarbamoyloxy)-4-phenyl-4-(3-(2-methoxyphenyl)-3-oxo-2-azaprop-1-yl)cyclo-hexane (trans-NPCO-DSC) was radiolabeled with tritium, and its binding characteristics to $K_v1.3$ channels were determined. Specific binding of [^{3}H]-trans-NPCO-DSC to $K_v1.3$ channels is a saturable, time-dependent, and fully reversible process. Saturation binding isotherms and competition binding experiments are consistent with the presence of two receptor sites for DSC derivatives on the $K_v1.3$ channel that display positive allosteric cooperativity. The high affinity interaction of [^{3}H]-trans-NPCO-DSC with $K_v1.3$ channels appears to correlate with the rates of C-type inactivation of the channel. These data, taken together, mark the first demonstration of the existence of multiple binding sites for an inhibitor of an ion channel and suggest that the high affinity interaction of trans-NPCO-DSC and similar inhibitors with $K_v1.3$ channels could be exploited for the development of selective molecules that target this protein.

The voltage-gated potassium channel, $K_v1.3$,[1] represents a therapeutic target for treating autoimmune diseases (*1*, *2*). $K_v1.3$ channels control the resting membrane potential of human T cells, and inhibition of these channels causes T cell depolarization, leading to an attenuation of the rise in intracellular Ca^{2+} concentration that occurs upon cell stimulation, which is required for T cell proliferation (*3*, *4*).

Although peptidyl blockers of $K_v1.3$ channels, such as margatoxin (MgTX) (*5*), *Stichodactyla helianthus* toxin (ShK) (*6*), and kaliotoxin (*7*) have immunosuppressant activity in vivo, efforts have been directed toward the identification of nonpeptidyl classes of selective $K_v1.3$ channel blockers. A number of small molecule inhibitors of $K_v1.3$, such as UK-78282 (*8*), WIN 17317-3 (*9*, *10*), verapamil (*11*, *12*), and correolide (*13*) have been described. Neither WIN 17317-3 nor verapamil appear to be viable drug development candidates since they block with high affinity voltage-gated sodium or calcium channels, respectively. The nortriterpene, correolide, isolated from the plant *Spachea correa*, is a potent and selective $K_v1.3$ channel blocker (*13*, *14*), and two analogues of correolide, with appropriate pharmacokinetic properties, suppress a delayed-type hypersensitivity response to tuberculin in vivo in mini-swine (*15*). However, the molecular complexity of correolide has hindered medicinal chemistry efforts to identify an analogue with the required characteristics for clinical development.

Recently, a novel class of potent $K_v1.3$ channel inhibitors that displays immunosuppressant activity in in vitro assays has been identified and characterized (*16*). The parent compound, 4-phenyl-4-(3-(2-methoxyphenyl)-3-oxo-2-aza-prop-1-yl)cyclohexanone (PAC), a disubstituted cyclohexyl (DSC) analogue, and a large number of analogues that include trans (down) and cis (up) isomers at the C-1 cyclohexyl position, display Hill coefficients for inhibition of near 2 in functional assays. Trans DSC derivatives are more potent inhibitors of ditritiocorreolide (diTC) binding to $K_v1.3$ than to native brain $K_v1.X$ channels. They also display other features that suggest that these compounds preferentially interact with channel conformations specific for $K_v1.3$ channels, which may be coupled to C-type inactivation.

* To whom correspondence should be addressed. Phone: (732) 594-7564. Fax: (732) 594-3925. E-mail: maria_garcia@merck.com.

[‡] Department of Ion Channels.

[§] Contributed equally to this work.

[||] Department of Drug Metabolism.

[⊥] Department of Medicinal Chemistry.

[1] Abbreviations: K_v, voltage-gated potassium channel; DSC, di-substituted cyclohexyl; PAC, 4-phenyl-4-(3-(2-methoxyphenyl)-3-oxo-2-azaprop-1-yl)cyclohexanone; trans-NPCO-DSC, *trans*-1-(*N*-*n*-propylcarbamoyloxy)-4-phenyl-4-(3-(2-methoxyphenyl)-3-oxo-2-azaprop-1-yl)cyclohexane; cis-NPCO-DSC, *cis*-1-(*N*-*n*-propylcarbamoyloxy)-4-phenyl-4-(3-(2-methoxyphenyl)-3-oxo-2-azaprop-1-yl)cyclohexane; trans-NiPCO-DSC, *trans*-1-(*N*-*i*-propylcarbamoyloxy)-4-phenyl-4-(3-(2-methoxyphenyl)-3-oxo-2-azaprop-1-yl)cyclohexane; cis-NiPCO-DSC, *cis*-1-(*N*-*i*-propylcarbamoyloxy)-4-phenyl-4-(3-(2-methoxyphenyl)-3-oxo-2-azaprop-1-yl)cyclohexane; diTC, ditritio-correolide; diHC, dihydrocorreolide; ^{125}I-HgTX$_1$A19Y/Y37F, monoiodotyrosine-hongotoxin$_1$-A19Y/Y37F; MgTX, margatoxin; ShK, *Stichodactyla helianthus* toxin; ChTX, charybdotoxin; IbTX, iberiotoxin; K_d, equilibrium dissociation constant; K_i, equilibrium inhibition constant for ligand, L.; K_e, equilibrium dissociation constant for effector, E.

10.1021/bi034122q CCC: $25.00
Published on Web 04/04/2003

In the present study, a *trans*-*N*-propylcarbamoyloxy analogue, *trans*-1-(*N*-*n*-propylcarbamoyloxy)-4-phenyl-4-(3-(2-methoxyphenyl)-3-oxo-2-azaprop-1-yl)cyclo-hexane (trans-NPCO-DSC), was radiolabeled with tritium, and its binding characteristics to $K_v1.3$ channels were determined. The results of these experiments are consistent with the presence of two channel receptor sites for DSC analogues that display positive allosteric cooperativity, illustrating for the first time the existence of multiple binding sites for an inhibitor on an ion channel. In addition, high affinity interaction of trans-NPCO-DSC with $K_v1.3$ channels appears to correlate with the rates of C-type inactivation of the channel. These data suggest that the high affinity interaction of trans-NPCO-DSC with $K_v1.3$ channels could serve as the basis for the development of more selective inhibitors of this channel that would display therapeutic utility.

EXPERIMENTAL PROCEDURES

Materials. Restriction enzymes and the pCI-neo vector were bought from Promega. The pEGFP-N1 vector was from Clontech, and *Pfu* DNA polymerase was from Stratagene. The TsA-201 cell line, a subclone of the human embryonic kidney cell line HEK293 that expresses the SV40 T antigen, was a gift of Dr. Robert DuBridge. All tissue culture media were from Gibco, serum was from Hyclone, and the FuGENE6 transfection reagent was from Roche. HEK293 cells stably transfected with either homotetrameric $K_v1.3$, or $K_v1.5$ channels were obtained from Prof. Olaf Pongs (Zentrum für Molekulare Neurobiologie, Hamburg, Germany), while HEK293 cells stably transfected with $K_v1.2$ were prepared as described (*17*). Correolide, diTC (29 Ci/mmol), and dihydrocorreolide (diHC) were prepared as previously described (*13*). Charybdotoxin (ChTX), iberiotoxin (IbTX), and ShK were purchased from Peptides International. MgTX was prepared as previously described (*18*). GF/C glass fiber filters were obtained from Whatman, and polyethylenimine was from Sigma. All other reagents were obtained from commercial sources and were of the highest purity commercially available.

Synthesis of [^{3}H]-Trans 1-(N-n-propylcarbamoyloxy)-4-phenyl-4-(3-(2-methoxyphenyl)-3-oxo-2-azaprop-1-yl)cyclohexane ([^{3}H]-trans-NPCO-DSC). A solution of 6 mg of *trans*-1-(*N*-allylcarbamoyloxy)-4-phenyl-4-(3-(2-methoxyphenyl)-3-oxo-2-azaprop-1-yl)cyclohexane in 0.8 mL of THF and 5 mg of 10% Pd/C were degassed and then reacted at room temperature with tritium gas. The reaction was stirred for 2 h, and any unreacted tritium gas was returned to the Tri-Sorber storage manifold. The catalyst was filtered with a 0.45 μm syringe filter (Gelman, #WAT200558) and then washed with 10 mL of ethanol. The solvent and labile tritium were rotoevaporated to near dryness. The dilution/evaporation procedure was repeated three times with about a total of 20 mL of ethanol. The dried residue was diluted with 2 mL of ethanol and subjected to HPLC chromatography (Zorbax RX-C_8, acetonitrile/water/TFA, 40:60:0.1). A total of 40 mCi of 99% radiochemically pure [^{3}H]-trans-NPCO-DSC) was obtained. The specific activity was calculated from the tracer solution count, determined by liquid scintillation counting, and tracer mass concentration, determined by UV spectroscopy using unlabeled compound to establish a calibration curve. The specific activity of [^{3}H]-trans-NPCO-DSC was 37.5 Ci/mmol.

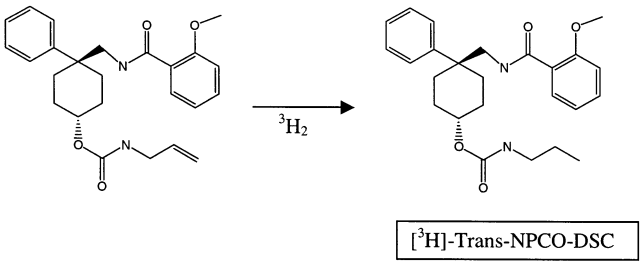

Binding of [^{3}H]-Trans-NPCO-DSC to $K_v1.3$. The interaction of [^{3}H]-trans-NPCO-DSC with membranes derived from HEK293 cells stably transfected with the $K_v1.3$ channel was monitored in a medium consisting of 135 mM NaCl, 4.6 mM KCl, 20 mM Tris-HCl, pH 7.4, 0.1% bacitracin. For saturation experiments, 15−20 μg of membranes were incubated in a total volume of 1 mL with increasing concentrations of [^{3}H]-trans-NPCO-DSC for 20 h at room temperature. To determine kinetics of ligand association, membranes were incubated with [^{3}H]-trans-NPCO-DSC for different periods of time at room temperature. Dissociation kinetics were initiated by addition of 3 μM trans-NPCO-DSC to membrane-bound [^{3}H]-trans-NPCO-DSC followed by incubation at room temperature for different periods of time. Competition experiments were carried out with [^{3}H]-trans-NPCO-DSC in the absence or presence of increasing concentrations of test compound. Separation of bound from free ligand was achieved by diluting samples with 4 mL of ice-cold buffer consisting of 100 mM NaCl, 20 mM Tris-HCl, pH 7.4, 0.1% Triton-X100. Samples were filtered through GF/C glass fiber filters that had been soaked in 0.5% polyethylenimine, and tubes were rinsed twice with 4 mL of ice-cold buffer. Triplicate samples were analyzed for each experimental point. Great care was taken to prevent use of certain plastics, such as polystyrene, because they can cause excessive sticking of ligand to the reaction vessel's surface.

Mutant Channel Constructs. A 9E10 *c-myc* tag was introduced at the C-terminus of $K_v1.3$ using an oligonucleotide cassette containing *Hind*III and *Not*I restriction sites. Site-directed mutagenesis was performed using the overlap extension technique (*19*). Polymerase chain reaction was carried out using proof reading *Pfu* DNA polymerase, and the integrity of all constructs was verified by nucleotide sequencing (automated sequencer, ABI 377).

Transfection of TsA-201 Cells and Membrane Preparation. The procedures for handling TsA-201 cells, their transfection with FuGENE6 transfection reagent, and preparation of membranes have been previously described (*20*). Membrane vesicles derived from HEK cells stably transfected with homo-multimeric Kv1.x channels were prepared as previously indicated (*16*). The final membrane pellet was resuspended in 100 mM NaCl, 20 mM Hepes-NaOH, pH 7.4. Aliquots were frozen in liquid N_2 and stored at −70 °C.

DiTC Binding. Binding of diTC to $K_v1.3$ membranes was carried out in a medium consisting of 135 mM NaCl, 4.6 mM KCl, 20 mM Tris-HCl, pH 7.4, 0.02% bovine serum albumin. Membranes were incubated in a total volume of 0.2 mL with increasing concentrations of diTC for 20 h at room temperature. Nonspecific binding was determined in the presence of 10 μM diHC. Separation of bound from free ligand was achieved using a filtration protocol as described (*13*, *16*). Triplicate samples were determined for each

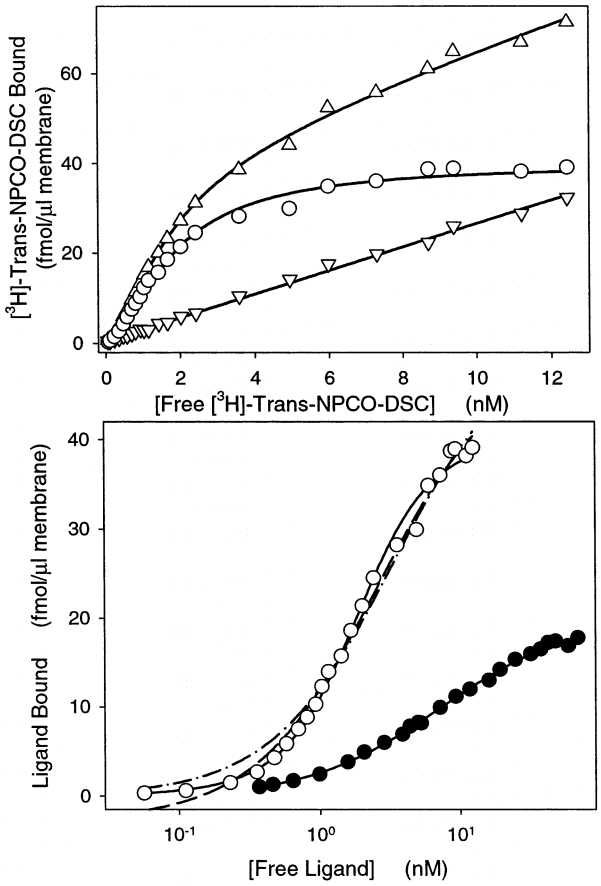

FIGURE 1: Binding of [^{3}H]-trans-NPCO-DSC to K_v1.3. Membranes prepared from HEK293 cells stably transfected with the K_v1.3 channel were incubated with increasing concentrations of either [^{3}H]-trans-NPCO-DSC (open symbols) or diTC (●) for 20 h at room temperature. The incubation media consisted of 135 mM NaCl, 4.6 mM KCl, 20 mM Tris-HCl, pH 7.4 and either 0.1% bacitracin (open symbols) or 0.02% bovine serum albumin (●). Separation of bound from free ligand was carried out by filtration techniques as described under Experimental Procedures. Upper panel: (△) total [^{3}H]-trans-NPCO-DSC binding, (▽) nonspecific binding determined in the presence of 3 μM of trans-NPCO-DSC, and (○) specific binding defined as the difference between total and nonspecific binding are presented. Specific [^{3}H]-trans-NPCO-DSC binding data in both panels have been fit to eq 8 (see Experimental Procedures and Appendix), corresponding to two identical binding sites with positive cooperativity. In the lower panel, the dashed line represents the fit to a one-site model where the parameters are left free, whereas in the dashed−dot line, the minimum value has been fixed to zero. The two-site model gives a better fit to the experimental [^{3}H]-trans-NPCO-DSC binding data. Trans-NPCO-DSC: α = 0.0628, K_d = 7.35 nM, B_{max} = 40.37 fmol/μL membrane; diTC: K_d = 7.45 nM, B_{max} = 20.39 fmol/μL membrane, nH = 0.89. The maximal binding of [^{3}H]-trans-NPCO-DSC is twice that of diTC.

experimental point. Standard deviation of the mean was typically less than 5%.

Data Analysis. Equilibrium binding data for saturation plots (Figure 1) were analyzed according to the two identical site saturation equation (Appendix, eq 8). Stimulation shown in positive homotropic or heterotropic equilibrium binding interactions (Figures 6−8) were analyzed by the normalized eqs 9 and 11 from the Appendix. Stimulation by effector, E, at various concentrations of ligand, L, was analyzed by simultaneous curve fitting of eq 11 as shown in the surface plot of Figure 5. Location and height of stimulation derived from the simultaneous curve fit of Figure 5 at limiting low ligand concentrations were determined by eqs 19 and 22 of the Appendix. Curve fits for association and dissociation experiments in Figures 2 and 3 were fit to simple bi- and monoexponential models, respectively, and were not based on two identical site positive homotropic cooperativity models. All curve fitting was performed in SigmaPlot 7.0 (SPSS Inc.).

RESULTS

Binding of [^{3}H]-Trans-NPCO-DSC to K_v1.3. It has previously been shown that trans-NPCO-DSC derivatives inhibit the K_v1.3 channel with Hill coefficients of near 2 in both functional assays and in competition binding experiments with diTC. These agents preferentially interact with K_v1.3 channel conformations related to C-type inactivation (*16*). To gain more insight into the properties of interaction of these inhibitors with the K_v1.3 channel, *trans*-1-(*N*-*n*-propylcarbamoyloxy)-4-phenyl-4-(3-(2-methoxyphenyl)-3-oxo-2-azaprop-1-yl)cyclohexane, (trans-NPCO-DSC), was radiolabeled with tritium. Under equilibrium conditions, binding of [^{3}H]-trans-NPCO-DSC to membranes derived from HEK-293 cells stably transfected with the K_v1.3 channel is saturable and displays a good signal-to-noise ratio (Figure 1, upper panel). The maximum receptor density, B_{max}, for this experiment is 40.4 fmol/μL membrane protein. In comparing the binding of [^{3}H]-trans-NPCO-DSC with that of diTC using a number of K_v1.3 membrane preparations, the B_{max} values for diTC binding are about half of those determined with [^{3}H]-trans-NPCO-DSC. In the example shown in Figure 1, lower panel, the B_{max} for diTC is 20.4 fmol/μL membrane protein, half that for NPCO-DSC in this same membrane preparation. Since it is well-established that diTC binds in a 1:1 stoichiometry to K_v1.3 channels (*13*), the data obtained with [^{3}H]-trans-NPCO-DSC strongly suggest a stoichiometry of two binding sites for this agent per homo-tetrameric K_v1.3 channel. The sigmoidicity of the specific binding of [^{3}H]-trans-NPCO-DSC shown in the saturation plot of Figure 1, upper panel, suggests that this binding is cooperative as well. The curve fit for this plot based on a two site model (eq 8, Appendix) gives a K_d of 7.4 nM for the initial binding, and a cooperativity coefficient (α) of 0.063, which results in an αK_d of 0.46 nM for binding of the second molecule. The average K_d of 6.98 ± 2.24 nM (n = 3) and the average α of 0.063 ± 0.031 (n = 3) indicate that binding of the first ligand molecule enhances the affinity of the channel for the second molecule by a factor of ca. 16. This is indicative of a strong positive allosteric coupling between sites.

Binding of [^{3}H]-Trans-NPCO-DSC to K_v1.3: Association and Dissociation Kinetics. The time-course of [^{3}H]-trans-NPCO-DSC association to K_v1.3 channels was determined next. Incubation of membranes with different concentrations of ligand (0.26, 0.72, 2.53, and 5.85 nM) results, in each case, in a time-dependent binding process that reaches equilibrium in about 6 h (Figure 2). Nonspecific binding, determined in the presence of 3 μM trans-NPCO-DSC, is time invariant and has been subtracted from the experimental points. The data at all ligand concentrations can be better fit to a biexponential process as compared to a monoexponential one, as illustrated by the analysis of the residuals (Figure 2, upper panel).

The kinetics of ligand dissociation were also determined. Dissociation of bound [^{3}H]-trans-NPCO-DSC was initiated

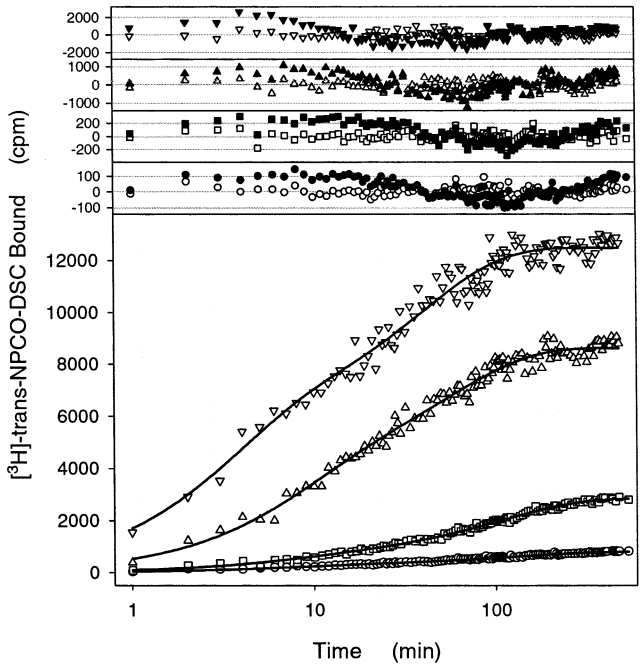

FIGURE 2: Binding of [^{3}H]-trans-NPCO-DSC to K_v1.3: association kinetics. Membranes prepared from HEK293 cells stably transfected with the K_v1.3 channel were incubated with 0.26 (○), 0.72 (□), 2.53 (△), or 5.85 nM (▽) [^{3}H]-trans-NPCO-DSC for different periods of time at room temperature. Other conditions are described under Experimental Procedures. Nonspecific binding, determined in the presence of 3 μM of trans-NPCO-DSC, is time-invariant and has been subtracted from the experimental points. Specific binding data have been fit to a biexponential process. Upper panel: analysis of residuals for mono- (closed symbols) or biexponential (open symbols) processes. The analysis of residuals shows that the difference between the estimated binding from the curve fit and the actual data is much less for the biexponential model than for the monoexponential model at each concentration of [^{3}H]-trans-NPCO-DSC tested.

by addition of excess, 3 μM trans-NPCO-DSC, and incubation was allowed to proceed at room temperature for different periods of time (Figure 3). The time-course of ligand dissociation follows monoexponential kinetics and is independent of the concentration of [^{3}H]-trans-NPCO-DSC used during the preincubation period, as expected for a first-order reaction. From these experiments, a dissociation rate constant, k_{-1}, of 0.0034 min^{-1}, corresponding to a $t_{1/2}$ of 202 min, was determined.

Binding of [^{3}H]-Trans-NPCO-DSC to K_v1.3: Effect of Different Potassium Channel Inhibitors. A number of structurally diverse classes of K_v1.3 inhibitors have been described. These include peptides such as ChTX (*21*), MgTX (*18*), and ShK (*22*) that bind with high affinity to the outer vestibule of the channel to physically occlude the pore, and small molecules, such as diHC (*13*), WIN 17317-3 (*9*, *10*), and verapamil (*12*), that appear to bind in the large water-filled cavity beneath the selectivity filter. Both diHC and WIN 17317-3 are state-dependent blockers of K_v1.3 and interact preferentially with the C-type inactivated form of the channel (*9*, *17*). As illustrated in Figure 4, left-hand panel, binding of [^{3}H]-trans-NPCO-DSC to K_v1.3 membranes is inhibited in a concentration-dependent manner by the K_v1.3 inhibitors ChTX, MgTX, and ShK but not by the homologous peptide, IbTX, that does not block K_v1.3 but is a selective blocker of the high-conductance, calcium activated potassium

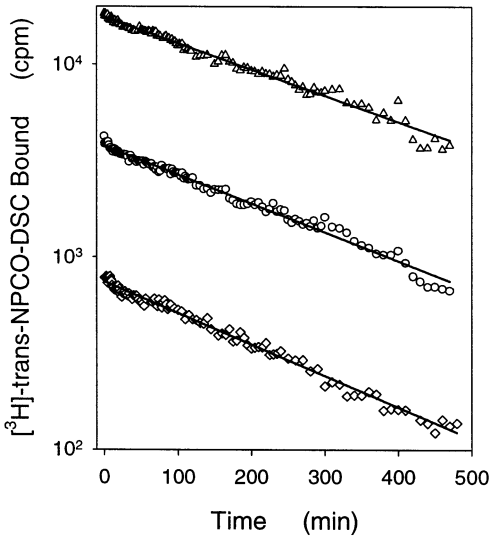

FIGURE 3: Binding of [^{3}H]-trans-NPCO-DSC to K_v1.3: dissociation kinetics. Membranes prepared from HEK293 cells stably transfected with the K_v1.3 channel were incubated with 0.29 (◇), 2.47 (○), or 12.3 nM (△) [^{3}H]-trans-NPCO-DSC, overnight at room temperature. Dissociation kinetics were initiated by addition of 3 μM trans-NPCO-DSC to membrane-bound [^{3}H]-trans-NPCO-DSC, followed by incubation at room temperature for different periods of time. Data have been fit to a single monoexponential decay corresponding to a first-order reaction. (◇) k_{-1} = 0.00375 min^{-1}; (○) k_{-1} = 0.00345 min^{-1}; and (△) k_{-1} = 0.00312 min^{-1}.

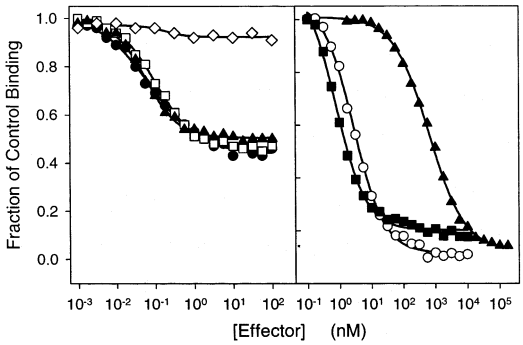

FIGURE 4: Binding of [^{3}H]-trans-NPCO-DSC to K_v1.3: effect of potassium channel inhibitors. Membranes prepared from HEK293 cells stably transfected with the K_v1.3 channel were incubated with 0.2 nM [^{3}H]-trans-NPCO-DSC in the absence or presence of increasing concentrations of either MgTX (□), ShK (▲), ChTX (●), or IbTX (◇) (left-hand panel) or WIN 17317-3 (■), diHC (○), or verapamil (▲) (right-hand panel) for 20 h at room temperature. Inhibition of binding was assessed relative to an untreated control. IC_{50} values: (●), 0.074 nM; (□), 0.104 nM; (▲), 0.058 nM; (○), 2.78 nM; (■), 0.77 nM; and (▲), 647 nM.

channel (*23*). The three peptides display similar potencies in the binding assay, K_i values of ~100 pM, and inhibition is partial, ca. 50%. Partial inhibition of binding by the peptides is expected since the preparation is a mix of outside-out and inside-out membranes, and the peptides only bind to outside-out facing channels. In contrast, inhibition of [^{3}H]-trans-NPCO-DSC binding by diHC, WIN 17317-3, and verapamil is almost complete with K_i values of 2.8, 0.77, and 647 nM, respectively (Figure 4, right-hand panel). It is important to note that the Hill coefficients for inhibition of [^{3}H]-trans-NPCO-DSC binding by these structurally diverse K_v1.3 inhibitors are close to 1. All these data suggest that the interaction of [^{3}H]-trans-NPCO-DSC with K_v1.3 membranes is a saturable and reversible process that displays

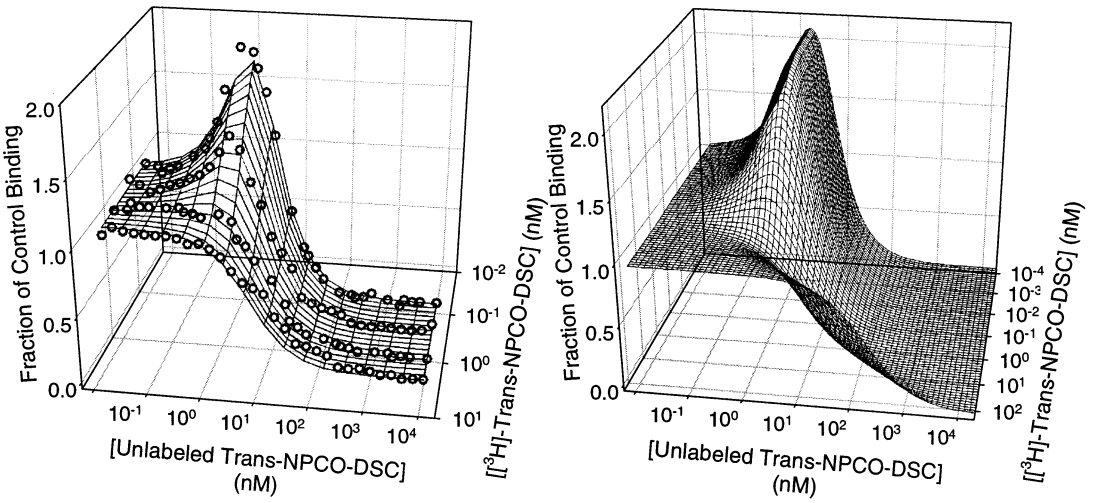

FIGURE 5: Binding of [^{3}H]-trans-NPCO-DSC to K_v1.3: positive cooperativity in the presence of trans-NPCO-DSC. Membranes prepared from HEK293 cells stably transfected with the K_v1.3 channel were incubated with (lowest to highest) 0.08, 0.31, 1.1, or 2.9 nM [^{3}H]-trans-NPCO-DSC, in the absence or presence of increasing concentrations of trans-NPCO-DSC, for 20 h at room temperature, as described under Experimental Procedures. Binding was assessed relative to an untreated control. Specific binding data have been fit to eq 11 (see Experimental Procedures and Appendix) corresponding to a two identical site model with positive cooperativity (left-hand panel). From this analysis, $K_d = 8.76 \pm 0.19$ nM and $\alpha = 0.061 \pm 0.0026$ were determined. The theoretical behavior of the two-site model according to the experimentally determined parameters is presented in the right-hand panel.

pharmacological properties expected from binding of ligand to the K_v1.3 channel.

Binding of [^{3}H]-Trans-NPCO-DSC to K_v1.3: Positive Cooperativity in the Presence of Trans-NPCO-DSC. Binding of [^{3}H]-trans-NPCO-DSC to K_v1.3 membranes was next evaluated in the absence or presence of increasing concentrations of trans-NPCO-DSC. When the concentration of [^{3}H]-trans-NPCO-DSC is low, ca. below 1 nM, increasing concentrations of unlabeled trans-NPCO-DSC causes stimulation of [^{3}H]-trans-NPCO-DSC binding followed, at higher trans-NPCO-DSC concentrations, by inhibition (Figure 5). These data, together with the data of Figure 1, can be explained by the existence of two identical binding sites that display positive cooperativity. At low concentrations of [^{3}H]-trans-NPCO-DSC, only one site in the channel will be occupied by ligand. Under these conditions, increasing but still low concentrations of unlabeled trans-NPCO-DSC will occupy the first site and stimulate binding of the labeled [^{3}H]-trans-NPCO-DSC to the second site. At much higher trans-NPCO-DSC concentrations, the unlabeled ligand begins to predominate in the second site as well, and only inhibition of [^{3}H]-trans-NPCO-DSC binding can occur. Solving a simple binding model for two identical site positive homotropic cooperativity (Figure 9, Model IB; Appendix) that describes this interaction of [^{3}H]-trans-NPCO-DSC interaction with K_v1.3 results in the normalized eq 11 from the Appendix:

$$B_e/B_{E=0} = [(\alpha K_d + [L] + [E])((\alpha K_d + [L])^2 + K_d{}^2(\alpha - \alpha^2))]/[(\alpha K_d + [L])((\alpha K_d + [L] + [E])^2 + K_d{}^2(\alpha - \alpha^2))]$$

This model predicts a stimulatory profile for unlabeled compound that depends on each concentration of labeled [^{3}H]-trans-NPCO-DSC used (right-hand panel, Figure 5). This surface plot from the normalized equation, generated with a wide range of concentrations of both labeled and unlabeled ligand, shows only a small region of stimulation, with maximal stimulation at the lowest labeled ligand concentration. The experimental data obtained at different [^{3}H]-trans-NPCO-DSC concentrations fit well to the predictions of the model (left-hand panel, Figure 5). The simultaneous curve fit used to generate the surface plot from these data gives a dissociation constant, K_d, of 8.8 nM, a cooperativity coefficient, α, of 0.061, and the second dissociation constant, αK_d, of 0.54 nM. These values are similar to those determined in the saturation binding experiments shown in Figure 1. As the ligand concentration approaches 0, the concentration of unlabeled ligand that gives maximal stimulation is 1.56 nM (from eq 19, Appendix), and the maximal amount of normalized stimulation is 2.08-fold (from eq 22, Appendix). Thus, for [^{3}H]-trans-NPCO-DSC, this model of two identical sites with positive homotropic cooperativity appears to closely match the data.

Binding of [^{3}H]-Trans-NPCO-DSC to K_v1.3: Effect of Cis- and Trans-DSC Isomers. Chemical modification of the parent compound, PAC, by reduction of the C-1 ketone in the A ring has generated trans (down) and cis (up) DSC isomer pairs. These isomers differ in the way they interact with the K_v1.3 channel (*16*): (1) while the K_v1.3 blocking activity of cis derivatives is insensitive to the nature of the *N*-carbamoyloxy substituent, there is a well-defined structure−activity relationship with the trans derivatives; (2) cis derivatives inhibit diTC binding to K_v1.3 and human brain membranes with equal potency, whereas trans derivatives are ~10-fold more potent inhibitors of diTC binding to K_v1.3; (3) cis derivatives have no effect on the interaction of ^{125}I-HgTX$_1$A19Y/Y37F with the outer vestibule of K_v1.x channels, but trans derivatives specifically modulate ^{125}I-HgTX$_1$A19Y/Y37F binding to K_v1.3 channels, and modulation of this binding correlates with rates of C-type inactivation of the channel. These observations suggest that specific channel conformations associated with C-type inactivation are responsible for the features of trans DSC isomer interactions with K_v1.3.

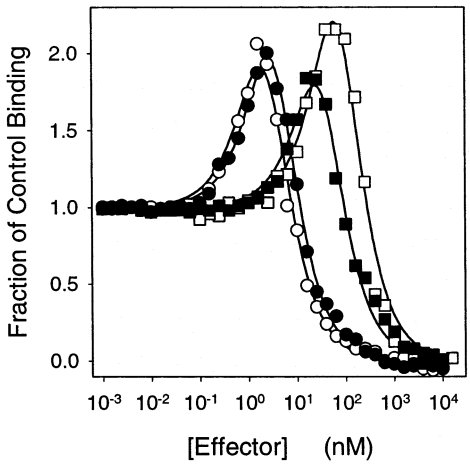

FIGURE 6: Binding of [^{3}H]-trans-NPCO-DSC to K_v1.3: effect of cis- and trans-DSC isomers. Membranes prepared from HEK293 cells stably transfected with the K_v1.3 channel were incubated with 0.083 nM [^{3}H]-trans-NPCO-DSC, in the absence or presence of increasing concentrations of either trans-NPCO-DSC (○), cis-NPCO-DSC (□), trans-NiPCO-DSC (●), or cis-NiPCO-DSC (■) for 20 h at room temperature. Binding was assessed relative to an untreated control. Specific binding data have been fit to eq 11 (see Experimental Procedures, Appendix) corresponding to a two identical site model with positive cooperativity, or to eq 9 (Appendix) corresponding to heterotropic cooperativity. For the heterotropic fit, α and K_d values from the homotropic fit are used and held constant. (○) K_d = 10.4 nM, α = 0.058; (□) K_e = 480 nM, β = 0.023, γ = 0.012; (●) K_e = 15.4 nM, β = 0.05, γ = 0.043; and (■) K_e = 127 nM, β = 0.05, γ = 0.031.

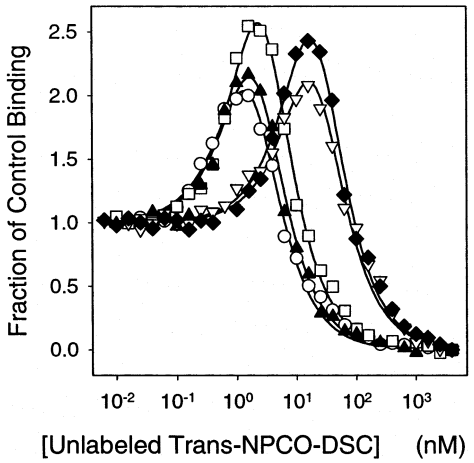

FIGURE 7: Binding of [^{3}H]-trans-NPCO-DSC to K_v1.3: role of C-type inactivation. Membranes derived from TsA-201 cells transiently transfected with either K_v1.3 (○), K_v1.3G375E (□), K_v1.3H399K (▲), K_v1.3H399T (▽), or K_v1.3G375Q (◆) were incubated with 0.1 nM [^{3}H]-trans-NPCO-DSC (○,□,▲) or 1 nM [^{3}H]-trans-NPCO-DSC (▽,◆) in the absence or presence of increasing concentrations of trans-NPCO-DSC, for 20 h at room temperature. Binding was assessed relative to an untreated control. Specific binding data have been fit to eq 11 (see Experimental Procedures, Appendix) corresponding to a two identical site model with positive cooperativity. (○) K_d = 10.04 nM, α = 0.033; (□) K_d = 18.88 nM, α = 0.023; (▲) K_d = 12.22 nM, α = 0.032; (▽) K_d = 109.15 nM, α = 0.040; and (◆) K_d = 173.35 nM, α = 0.015.

To determine the mechanism of interaction of DSC isomers, [^{3}H]-trans-NPCO-DSC binding experiments similar to those described in Figure 5 were carried out in the presence of increasing concentrations of cis-NPCO-DSC, as well as in the presence of the analogues, cis- or trans-NiPCO-DSC. Data from these experiments are presented in Figure 6. Both isomers display similar characteristics as modulators of [^{3}H]-trans-NPCO-DSC binding to K_v1.3, and the calculated K_e values, 480 nM for cis-NPCO-DSC and 15.4 and 127 nM for trans and cis-NiPCO-DSC derivatives, are similar to the K_i values (80, 10, and 125 nM, respectively) determined in diTC binding experiments with K_v1.3 membranes. Other pairs of isomers gave identical results as those seen in Figure 6, although the concentrations needed to produce the effects are different for each compound (data not shown). These data suggest that although trans-isomers can be distinguished in their interaction with K_v1.3 channels, cis-isomers most likely bind at that same site on the channel.

Binding of [^{3}H]-Trans-NPCO-DSC to K_v1.3: Role of C-Type Inactivation. We have previously shown that modulation of ^{125}I-HgTX$_1$A19Y/Y37F binding to K_v1.3 by trans-DSC isomers correlates with the rates of C-type inactivation of the channel (*16*). Single point mutations that change the rates of C-type inactivation also modify the allosteric coupling between the sites where peptides and trans-isomers bind. To determine the consequences of C-type inactivation on binding of [^{3}H]-trans-NPCO-DSC to K_v1.3 channels, mutants with altered kinetics of inactivation were evaluated. K_v1.3(Gly^{375}Glu) and K_v1.3(His^{399}Lys) display similar rates of C-type inactivation as the wild-type channel, while K_v1.3(His^{399}Thr), K_v1.3(His^{399}Tyr), and K_v1.3(Gly^{375}Gln) inactivate slower than native channels (ref *16* and data not shown). Results of binding experiments with these channels are presented in Figure 7. Both K_v1.3(Gly^{375}Glu) and K_v1.3(His^{399}Lys) mutants bind [^{3}H]-trans-NPCO-DSC with similar dissociation constants, 18.88 and 12.22 nM, respectively, and cooperativity coefficients as those found with the wild-type channel. With the slower inactivating mutants K_v1.3(His^{399}Thr) and K_v1.3(Gly^{375}Gln), the concentration of unlabeled trans-NPCO-DSC at which maximum stimulation of binding occurs is higher than with the wild-type channel. The K_d values for these mutants are 109 and 173 nM, respectively, about 10−20-fold higher than for K_v1.3, and similar data were obtained with K_v1.3(His^{399}Tyr) (data not shown). These data indicate that a correlation exists between the affinity of [^{3}H]-trans-NPCO-DSC and the rates of C-type inactivation of the channel and predicts a mechanism by which trans-isomers display specificity for K_v1.3 versus other K_v1.x channels that do not C-type inactivate.

Binding of [^{3}H]-Trans-NPCO-DSC to K_v1.x Channels. The properties of [^{3}H]-trans-NPCO-DSC binding to other, non-inactivating, K_v1.x channels have also been determined. For these experiments, we investigated homo-multimeric K_v1.2 and K_v1.5 channels stably expressed in HEK293 cells. Binding of [^{3}H]-trans-NPCO-DSC to membranes derived from these cell lines cannot be detected under the low ligand concentration protocols of Figure 5, despite similar levels of channel expression to those of K_v1.3, as determined independently from experiments employing diTC as the ligand (*17*). At concentrations of [^{3}H]-trans-NPCO-DSC around 1 nM, the effect of increasing trans-NPCO-DSC concentrations is similar to that previously seen with K_v1.3 channels, although the concentrations of ligand needed to produce the characteristic modulation of binding are different (Figure 8). From these experiments, K_d values were determined to be 148 and 80 nM and α parameters 0.029 and

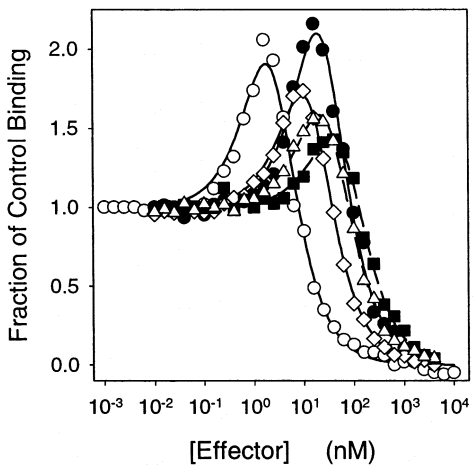

FIGURE 8: Binding of [^{3}H]-trans-NPCO-DSC to K_v1.2 and K_v1.5. Membranes prepared from HEK293 cells stably transfected with K_v1.2 (●) (50 μg) or K_v1.5 (◇,△,■) (35 μg) were incubated, in a total volume of 0.2 mL, with 2 nM [^{3}H]-trans-NPCO-DSC, in the absence or presence of increasing concentrations of either trans-NPCO-DSC (●,◇), trans-NiPCO-DSC (△), or cis-NiPCO-DSC (■) for 20 h at room temperature. Binding was assessed relative to an untreated control. Specific binding data have been fit to eq 11 (see Experimental Procedures, Appendix) corresponding to a two identical site model with positive cooperativity or to eq 9 (Appendix) corresponding to heterotropic cooperativity, with α and K_d held constant at control levels for K_v1.5. Data from experiments carried out with K_v1.3 membranes (○) (Figure 6) are also presented for comparison. (○) K_d = 10. 35 nM, α = 0.058; (●) K_d = 148.29 nM, α = 0.029; (◇) K_d = 80.1 nM, α = 0.03; (△) K_e = 172 nM, β = 0.031, γ = 0.036; and (■) K_e = 297 nM, β = 0.042, γ = 0.047.

0.030 for K_v1.2 and K_v1.5, respectively. The effect of trans- and cis-NiPCO-DSC derivatives on [^{3}H]-trans-NPCO-DSC binding to K_v1.5 was also evaluated (Figure 8). Both isomers display similar characteristics as modulators of [^{3}H]-trans-NPCO-DSC binding to K_v1.5, with K_e values of 297 and 172 nM for the cis- and trans-derivatives, respectively. The K_e value of the cis-derivative for K_v1.5 channels, 297 nM, is <2.5-fold that of the same compound on the K_v1.3 channel, 127 nM. However, for the trans-derivative the differences in K_e values between these two channels, 172 and 15.4 nM, is >10-fold. These data are all consistent with the observation that trans-isomers show a degree of specificity in their interaction with the K_v1.3 channel and that this specificity is derived from an intrinsic higher affinity site in the channel for this ligand. In addition, the affinity of the receptor can be modulated according to the rates of C-type inactivation of the channel. Consistent with this, [^{3}H]-trans-NPCO-DSC binding to C-type inactivating K_v1.4 channels displays identical K_d and α parameters as those determined for K_v1.3 (data not shown).

DISCUSSION

The results reported in this study represent the first characterization of the binding properties of [^{3}H]-trans-NPCO-DSC with K_v1.3 channels. This compound belongs to the di-substituted cyclohexyl family of K_v1.3 channel blockers that inhibit human T cell activation processes in in vitro assays and represents a new class of immunosuppressant agents (*16*). The major findings in this study concern the identification of two identical binding sites on the K_v1.3 channel for DSC that display positive cooperativity and the correlation between [^{3}H]-trans-NPCO-DSC binding affinity and rates of C-type inactivation of the channel. All these data are consistent with previous observations made with this class of compounds. Both the parent compound, PAC, and the cis- and trans-DSC derivatives have been shown to display Hill coefficients of near two in functional channel assays, as well as in other in vitro assays, suggesting that more than one molecule of inhibitor contributes to the measured activity. In electrophysiological recordings of K_v1.3 channels from human T cells, the kinetics of channel block by PAC also suggest the involvement of more than one molecule in eliciting channel block. Thus, data combined from different assays and from direct stoichiometric measurements provide strong evidence for the existence of multiple binding sites in the homo-tetrameric K_v1.3 channel.

The strongest argument for the existence of two binding sites for this class of inhibitors has been obtained from saturation binding experiments with [^{3}H]-trans-NPCO-DSC. Binding of the ligand occurs with a good signal-to-noise ratio to K_v1.3 membranes, allowing a very accurate determination of the maximum density of receptors present in the preparation. When these data are compared to those obtained in the same preparations where diTC binding is monitored, it is clear that the relative stoichiometry for [^{3}H]-trans-NPCO-DSC/diTC is 2:1. It has previously been established that diTC and peptidyl inhibitors of the channel, such as MgTX, bind in a 1:1 stoichiometry to the channel (*13*). Since it is known that only one molecule of peptide can bind to the channel (*24*), all the data are consistent with the presence of two sites for [^{3}H]-trans-NPCO-DSC and its analogues on the K_v1.3 channel. Another strong piece of evidence for the existence of multiple sites for [^{3}H]-trans-NPCO-DSC has been obtained from experiments such as those illustrated in Figures 5−8. The observation that binding of [^{3}H]-trans-NPCO-DSC stimulated in the presence of unlabeled ligand is not consistent with the existence of a single binding site for these compounds since in this case a single monophasic inhibition curve would have been obtained. The enhancement of binding that occurs at low concentrations of [^{3}H]-trans-NPCO-DSC can be easily explained if one assumes the existence of two binding sites for inhibitor where occupancy of the first site enhances the affinity of the second by a cooperativity factor α. Using this simple model, we solved the binding equations and demonstrated a good fit to the experimental data. The data predict that the affinity of the ligand for the second site in K_v1.3 is enhanced about 20-fold after the first site has been occupied and illustrates the importance of exploring ligand−receptor interactions under a wide range of conditions. For instance, stimulation of [^{3}H]-trans-NPCO-DSC binding is not observed at high ligand concentration, which is fully consistent with our two site-cooperativity model.

Although the experimental data do not demand that the binding sites be identical, we favor this alternative because of the tetrameric arrangement of homomeric subunits, which is assumed to be symmetrical. Initially, there are four potential binding sites. Once the compound is bound to the first site, experimental data (Figure 1) indicate that only one additional site is then available. Mathematically, this binding sequence is reduced to a two identical site model.

Although other structural classes of small molecule inhibitors of potassium channels, such as correolide, verapamil, and WIN 17317-3, have been described, there is no evidence for the existence of multiple binding sites for these agents. The stoichiometry of correolide analogues has been well-established with the use of diTC (*13*, *24*), but no direct measurements of binding have yet been made with the other inhibitors. However, the monotonic pattern of inhibition, with no stimulation of [^{3}H]-trans-NPCO-DSC binding, is more consistent with the presence of a single binding site for these agents.

Chemical modification of the parent compound, PAC, at the C-1 ketone group led to the production of cis- and trans-DSC derivatives, and the radioligand used in the present study, [^{3}H]-trans-NPCO-DSC, belongs to the trans-class of isomers. Several features distinguish these compounds in their interaction with the K_v1.3 channel (*16*). The potency of cis-isomers as inhibitors of diTC binding to K_v1.3 and human brain K_v1.x channels is identical, but trans-isomers are about 10-fold more potent inhibitors of diTC binding to K_v1.3. In functional assays, cis-isomers are not very sensitive to the chain substitution, while in marked contrast, trans-isomers only tolerate small alkyl chain substitutions. Finally, only trans-isomers can allosterically couple with the receptor in the outer vestibule where peptide inhibitors bind, and this interaction correlates with the rates of C-type inactivation of K_v1.3. Since all these data indicate that trans-DSC compounds preferentially interact with K_v1.3 channels, it was of interest to determine the modulation of [^{3}H]-trans-NPCO-DSC binding by cis-DSC isomers. These experiments illustrate that, although the cis-isomers exert their effects at higher concentrations, both types of isomers appear to cause about the same level of binding stimulation, suggesting that they share a common receptor site on the channel. This idea is also consistent with a previous observation in which the potency of trans-NPCO-DSC as an inhibitor of ^{125}I-HgTX$_1$-A19Y/Y37F binding to K_v1.3 was shifted to lower affinity in the presence of concentrations of cis-NPCO-DSC that, by themselves, do not affect peptide binding (*16*).

It has previously been reported that C-type inactivation confers a high affinity interaction of certain inhibitors with the K_v1.3 channel. Thus, agents such as correolide (*15*, *17*, *25*)], UK-78,282 (*8*), and WIN-17317−3 (*9*) preferentially associate with this state of the channel, and mutations that alter the rates of channel inactivation have a profound effect on kinetics of inhibitor block and potency. These compounds are thought to bind in a region of the protein that is part of the large water-filled cavity underneath the selectivity filter (*8*, *26*). C-type inactivation, however, has been shown to involve large conformational changes in the outer vestibule of the channel (*27*, *28*). Thus, it appears that those conformational changes in the outer region of the channel are translated to other more distant regions of the protein that are involved in ion conduction. C-type inactivation also plays an important role in the interaction of [^{3}H]-trans-NPCO-DSC with K_v1.3. Single point mutations in the outer pore region of the channel that slow rates of channel inactivation cause a marked decrease in [^{3}H]-trans-NPCO-DSC affinity, whereas mutations at the same positions that do not affect inactivation have no significant effect. In addition, [^{3}H]-trans-NPCO-DSC binding to other K_v1.x channels, such as K_v1.2 and K_v1.5, occurs with lower affinity than to K_v1.3, consistent with the fact that the inactivation process in these channels is much reduced. All these data, taken together, suggest a molecular mechanism that leads to specificity of inhibitor interaction with K_v1.3 channels.

Although the site of interaction of DSC analogues in the channel has not been mapped in detail, there are several lines of evidence that suggest that these compounds also bind in a region that encompass the water cavity of the channel. Thus, compounds can access their binding sites from the intracellular compartment (*16*), and other inhibitors such as correolide, WIN17317-3, and verapamil compete for binding of [^{3}H]-trans-NPCO-DSC to the channel. Given that this region of the channel is 100% identical within K_v1.1−1.6 channels, channel specificity must be derived from conformational changes resulting from specific gating processes. In this manner, C-type inactivation provides a very selective feature since this process is only shared with K_v1.3 by one other channel, K_v1.4.

What are the molecular mechanisms that contribute to positive cooperativity in the interaction of [^{3}H]-trans-NPCO-DSC with K_v1.3 and other K_v1.x channels? Our data suggest a large shift, ca. 20-fold, in affinity after binding of the first molecule has occurred. Such a change could be the consequence of either the first molecule favoring access of the second one, or the second one stabilizing binding of the first ligand, or a combination of both effects. Although we have not observed differences in ligand dissociation rates after incubation with different concentrations of [^{3}H]-trans-NPCO-DSC, this could be due to the fact that these experiments are initiated by addition of excess of unlabeled ligand that will lead to immediate occupancy of all sites. On the other hand, the time-course of ligand association is better fit to a biexponential process. Given the complexity of the kinetic model, we have not determined the theoretical behavior for the time-dependence of ligand association. The stoichiometry of binding clearly indicates that two molecules of [^{3}H]-trans-NPCO-DSC can bind to the channel. This constraint implies that the channel subunits where inhibitor binds must be diagonally oriented and that binding does not occur within adjacent subunits.

There are very limited examples of binding behavior in the literature that resemble those of [^{3}H]-trans-NPCO-DSC with K_v1.3. However, as discussed above and confirmed by experimental data, binding conditions, such as ligand and receptor concentrations, can be critical for illustrating the positive cooperativity between sites. We do not know if this situation is unique to the class of DSC inhibitors. On the whole, features of the specific interaction of the trans-DSC isomers with the K_v1.3 channel strongly suggest that it may be possible to identify further agents within this structural series that could be developed as therapeutically useful immunosuppressants.

APPENDIX

The model that we have used to describe the stimulation of binding of low concentrations of [^{3}H]-NPCO-DSC by unlabeled ligand to K_v1 series potassium channels is based upon utilizing all terms in the binding equation for positive homotropic cooperative interactions. There are two simplifications: the first is based on experimental data that show the presence of two binding sites for [^{3}H]-Trans-NPCO-DSC;

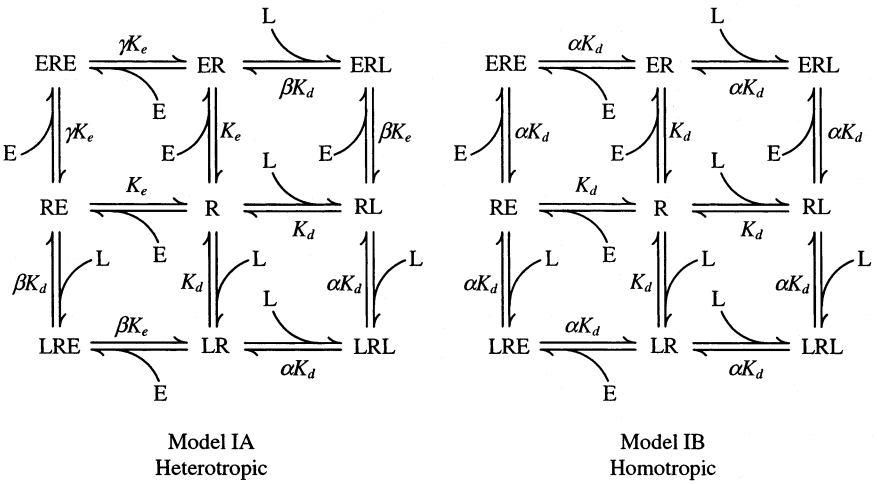

FIGURE 9: State diagram showing interactions leading to positive heterotropic cooperativity and positive homotropic cooperativity in a two identical site binding model. Receptor, R, Ligand, L, and Effector, E interact through equilibrium binding dissociation constants, K_d and K_e, and cooperativity coefficients, α, β, and γ.

the second one presumes that these two binding sites are identical for initial binding, which is described by K_d, and that binding to the allosterically modified second site can be described by αK_d. The resultant binding equation adequately describes a region of stimulation by an effector molecule at low ligand concentrations. An additional novel part of the development is the modeling from the first derivative of the location and height of the stimulation at limiting labeled ligand concentration.

The development begins with the general model for heterotropic interaction at two sites shown in Figure 9, left panel. The lower right quadrant shows the interaction of the labeled ligand, L, with the receptor, R, at two identical sites with a dissociation constant, K_d. Interaction with the second site is modified through allosteric interaction coefficient, α, and results in the dissociation constant, αK_d. An effector, E, can bind similarly with an initial dissociation constant, K_e, followed by the constant γK_e for the second site. When the ligand, L, is bound to the first site, the effector, E, can bind to the second site with an allosteric interaction coefficient of β, giving a dissociation constant of βK_e for this interaction and of βK_d for the converse interaction of L with RE.

Because of the 4-fold symmetry of voltage-gated potassium channels, formally, there are four initial binding sites available. However, because empirically only two molecules of the ligand can bind at any one time, all models reduce to two identical sites. This configuration results in the symmetry shown in the model (Figure 9, left panel). When the effector is the unlabeled version of the labeled ligand, the dissociation constant K_e becomes equal to K_d, and all of the allosteric interaction constants become the same, equal to α.

For the heterotropic model there are six symmetrical pairs of equilibria, two for the initial binding and four for the secondary. Examples of each type are shown in eqs 1 and 2.

$$K_d = \frac{[R][L]}{[RL]} \Rightarrow [RL] = \frac{[R][L]}{[K_d]} \quad (1)$$

$$\beta K_e = \frac{[RL][E]}{[ERL]} \Rightarrow [ERL] = \frac{[RL][E]}{[\beta K_e]} = \frac{[R][L][E]}{\beta K_e K_d} \quad (2)$$

The total bound species of ligand, B, divided by the total receptor species, R_T, is shown in the next equation:

$$\frac{B}{R_T} = \frac{[RL] + [LR] + 2[LRL] + [LRE] + [ERL]}{[R] + [RL] + [LR] + [LRL] + [RE] + [ER] + [ERE] + [LRE] + [ERL]} \quad (3)$$

Note that when measuring the LRL species, the ligand, L, is present twice; therefore, each [LRL] must be counted twice to obtain the [L] bound to that species. This explanation is why the 2[LRL] term appears in the numerator for bound species.

After substituting the various terms for their equilibria, setting B_{max} for two binding sites to $2R_T$, and factoring out secondary common denominators and other common terms, the equation for binding, B_E, in the presence of effector is:

$$B_E = \frac{B_{max}[L]K_e\gamma(\alpha\beta K_e K_d + \beta[L]K_e + \alpha[E]K_d)}{\alpha\beta\gamma(K_e^2K_d^2 + 2[L]K_e^2K_d + 2[E]K_eK_d^2) + \beta\gamma[L]^2K_e^2 + \alpha\beta[E]^2K_d^2 + 2\alpha\gamma[E][L]K_eK_d} \quad (4)$$

This initial model development is based on the positive heterotropic interaction expected for a molecule different from the ligand. The level of dependency for curve fitting for the heterotropic model would be high, near 1, for most molecules related to the original ligand because the level of cooperativity would be expected to be similar. Therefore, curve fitting equations actually used for heterotropic interactions depend on using the values for K_d and α determined from the homotropic data and calculate a K_e for the effector plus the β and γ cooperativity coefficients. In addition, as shown by similar peak heights, which at limiting ligand concentrations depend only on the cooperativity coefficients (see below) for compounds very closely related to the ligand, the level of cooperativity will be approximately the same, and α can replace β and γ.

$$B_E = [B_{max}[L]K_e(\alpha K_e K_d + [L]K_e + [E]K_d)]/[\alpha K_e^2 K_d^2 + 2\alpha[L]K_e^2 K_d + [L]^2 K_e^2 + 2\alpha[E]K_e K_d^2 + [E]^2 K_d^2 + 2[E][L]K_e K_d] \quad (5)$$

This equation can be grouped to simplify partial derivative calculation and to calculate the position and height of the stimulation (see below). Eq 6 happens to be equivalent to a rearrangement of an equation describing the homotropic cooperative binding of the retinal rod G protein, transducin, to rhodopsin (eq 3 in ref *29*).

$$B_E = \frac{B_{max}[L]K_e(\alpha K_e K_d + [L]K_e + [E]K_d)}{(\alpha K_e K_d + [L]K_e + [E]K_d)^2 + K_e^2 K_d^2(\alpha - \alpha^2)} \quad (6)$$

For homotropic cooperativity where the effector is the unlabeled ligand, $K_e = K_d$, the equation reduces to

$$B_E = \frac{B_{max}[L](\alpha K_d + [L] + [E])}{(\alpha K_d + [L] + [E])^2 + K_d^2(\alpha - \alpha^2)} \quad (7)$$

In the presence of no effector, E, the equation reduces to the standard two site cooperative binding model

$$B_{E=0} = \frac{B_{max}[L](\alpha K_d + [L])}{(\alpha K_d + [L])^2 + K_d^2(\alpha - \alpha^2)} \quad (8)$$

To reduce the number of parameters, binding in the presence of a heterotropic effector (eq 4) can be normalized by dividing by this basic equation with no effector (eq 8).

$$\frac{B_E}{B_{E=0}} = [\gamma K_e(([L] + \alpha K_d)^2 + K_d^2(\alpha - \alpha^2))(\alpha\beta K_e K_d + \beta[L]K_e + \alpha[E]K_d)]/[([L] + \alpha K_d)(\alpha\beta\gamma(K_e^2 K_d^2 + 2[L]K_e^2 K_d + 2[E]K_e K_d^2) + \beta\gamma L^2 K_e^2 + \alpha\beta[E]^2 K_d^2 + 2\alpha\gamma[E][L]K_e K_d)] \quad (9)$$

Similarly, for simplified heterotropic cooperativity, the equation is

$$\frac{B_E}{B_{E=0}} = \frac{K_e(\alpha K_e K_d + [L]K_e + [E]K_d)((\alpha K_d + [L])^2 + K_d^2(\alpha - \alpha^2))}{((\alpha K_d + [L])((\alpha K_e K_d + [L]K_e + [E]K_d)^2 + K_e^2 K_d^2(\alpha - \alpha^2)))} \quad (10)$$

For homotropic cooperativity, the equation is

$$\frac{B_E}{B_{E=0}} = \frac{(\alpha K_d + [L] + [E])((\alpha K_d + [L])^2 + K_d^2(\alpha - \alpha^2))}{((\alpha K_d + [L])((\alpha K_d + [L] + [E])^2 + K_d^2(\alpha - \alpha^2)))} \quad (11)$$

Homotropic interactions use the above-described substitutions for limiting low concentrations of ligand. Homotropic interactions for higher ligand concentrations are fit to simultaneous multiple data sets that must include a low ligand concentration set. Single curve fits at moderate and higher ligand concentrations where there is reduced or no significant stimulatory peak collapse because terms with α or K_d in them diminish in their influence.

At higher ligand concentrations, there is no stimulation, and the α containing terms drop out both for the heterotropic (eq 12) and the homotropic (eq 13) interactions. As can be seen for the homotropic interaction, the K_d terms cancel as well, and the binding depends simply on the effector, E, and on the ligand, L.

$$\frac{B_E}{B_{E=0}} = \frac{[L]K_e([L]K_e + [E]K_d)}{([L]K_e + [E]K_d)^2} = \frac{[L]K_e}{[L]K_e + [E]K_d} \quad (12)$$

$$\frac{B_E}{B_{E=0}} = \frac{[L]}{[L] + [E]} = \frac{1}{1 + \frac{[E]}{[L]}}$$

To determine the concentration of E at which there is maximum stimulation, the first derivative is taken, and the numerator is set to zero as shown in eqs 14 and 15.

$$\frac{\partial B_E}{\partial E} = [K_e K_d(\alpha K_d + [L])((\alpha K_e K_d + [L]K_e + [E]K_d)^2 + K_e^2 K_d^2(\alpha - \alpha^2))((\alpha K_d + [L])^2 + K_d^2(\alpha - \alpha^2)) - 2K_e K_d(\alpha K_d + [L])((\alpha K_d + [L])^2 + K_d^2(\alpha - \alpha^2)) \times (\alpha K_e K_d + [L]K_e + [E]K_d)^2]/[(\alpha K_d + [L])((\alpha K_e K_d + [L]K_e + [E]K_d)^2 + K_e^2 K_d^2(\alpha - \alpha^2))^2] \quad (14)$$

$$\text{Num} = 0 = (\alpha K_d + [L]K_e + [E]K_d)^2 + K_e^2 K_d^2(\alpha - \alpha^2) - 2(\alpha K_d + [L]K_e + [E]K_d)^2 \quad (15)$$

Solving for the concentration of effector that produces maximum heterotropic stimulation, E_{max}, gives the solution shown in the following general and limiting equations:

$$E_{max} = K_e\left(\sqrt{\alpha - \alpha^2} - \alpha - \frac{[L]}{K_d}\right) \quad (16)$$

$$\lim_{[L]\to 0} E_{max} = K_e(\sqrt{\alpha - \alpha^2} - \alpha) \quad (17)$$

The E_{max} for homotropic interaction has these general and limiting equations.

$$E_{max} = K_d(\sqrt{\alpha - \alpha^2} - \alpha) - [L] \quad (18)$$

$$\lim_{[L]\to 0} E_{max} = K_d(\sqrt{\alpha - \alpha^2} - \alpha) \quad (19)$$

The maximal level of stimulation can be obtained by calculating the normalized binding $B_E/B_{E=0}$ (eq 9) at E_{max} (eq 15)

$$\frac{B_E}{B_{E=0}} = \frac{K_e^2 K_d\sqrt{\alpha - \alpha^2}((\alpha K_d + [L])^2 + K_d^2(\alpha - \alpha^2))}{(\alpha K_d + [L])((K_e K_d\sqrt{\alpha - \alpha^2})^2 + K_e^2 K_d^2(\alpha - \alpha^2))} \quad (20)$$

All K_e terms drop out, and there is no difference between homotropic and heterotropic interactions for this peak height

calculation, under the condition that all cooperativity coefficients are equal to α.

$$\frac{B_E}{B_{E=0}} = \frac{(\alpha K_d + [L])^2 + K_d{}^2(\alpha - \alpha^2)}{2K_d(\alpha K_d + [L])\sqrt{\alpha - \alpha^2}} \qquad (21)$$

As the ligand, L, concentration approaches 0, all dissociation constants drop out, and the maximal stimulation becomes a simple function of α.

$$\lim_{[L]\to 0} \frac{B_E}{B_{E=0}} = \frac{1}{2\sqrt{\alpha - \alpha^2}} \qquad (22)$$

ACKNOWLEDGMENT

We thank Dr. MacHardy Smith for helpful comments and discussions during the course of this study. We also thank Dr. Ana-Rosa Linde-Arias and Brian Green for experimental support.

REFERENCES

1. Cahalan, M. D., and Chandy, K. G. (1997) *Curr. Opin. Biotechnol. 8*, 749−756.
2. Kaczorowski, G., and Koo, G. C. (1994) *Perspect. Drug. Discovery Des. 2*, 233.
3. Leonard, R. J., Garcia, M. L., Slaughter, R. S., and Reuben, J. P. (1992) *Proc. Natl. Acad. Sci. U.S.A. 89*, 10094−10098.
4. Lin, C. S., Boltz, R. C., Blake, J. T., Nguyen, M., Talento, A., Fischer, P. A., Springer, M. S., Sigal, N. H., Slaughter, R. S., Garcia, M. L., Kaczorowski, G. J., and Koo, G. C. (1993) *J. Exp. Med. 177*, 637−645.
5. Koo, G. C., Blake, J. T., Talento, A., Nguyen, M., Lin, S., Sirotina, A., Shah, K., Mulvany, K., Hora, D., Jr., Cunningham, P., Wunderler, D. L., McManus, O. B., Slaughter, R., Bugianesi, R., Felix, J., Garcia, M., Williamson, J., Kaczorowski, G., Sigal, N. H., Springer, M. S., and Feeney, W. (1997) *J. Immunol. 158*, 5120−5128.
6. Beeton, C., Wulff, H., Barbaria, J., Clot-Faybesse, O., Pennington, M., Bernard, D., Cahalan, M. D., Chandy, K. G., and Beraud, E. (2001) *Proc. Natl. Acad. Sci. U.S.A. 98*, 13942−13947.
7. Beeton, C., Barbaria, J., Giraud, P., Devaux, J., Benoliel, A.-M., Gola, M., Sabatier, J. M., Bernard, D., Crest, M., and Beraud, E. (2001) *J. Immunol. 166*, 936−944.
8. Hanson, D. C., Nguyen, A., Mather, R. J., Rauer, H., Koch, K., Burgess, L. E., Rizzi, J. P., Donovan, C. B., Bruns, M. J., Canniff, P. C., Cunningham, A. C., Verdries, K. A., Mena, E., Kath, J. C., Gutman, G. A., Cahalan, M. D., Grissmer, S., and Chandy, K. G. (1999) *Br. J. Pharmacol. 126*, 1707−1716.
9. Nguyen, A., Kath, J. C., Hanson, D. C., Biggers, M. S., Canniff, P. C., Donovan, C. B., Mather, R. J., Bruns, M. J., Rauer, H., Aiyar, J., Lepple-Wienhues, A., Gutman, G. A., Grissmer, S., Cahalan, M. D., and Chandy, K. G. (1996) *Mol. Pharmacol. 50*, 1672−1679.
10. Hill, R. J., Grant, A. M., Volberg, W., Rapp, L., Faltynek, C., Miller, D., Pagani, K., Baizman, E., Wang, S., Guiles, J. W., and Krafte, D. S. (1995) *Mol. Pharmacol. 48*, 98−104.
11. Chandy, K. G., DeCoursey, T. E., Cahalan, M. D., McLaughlin, C., and Gupta, S. (1984) *J. Exp. Med. 160*, 369−385.
12. Rauer, H., and Grissmer, S. (1996) *Mol. Pharmacol. 50*, 1625−1634.
13. Felix, J. P., Bugianesi, R. M., Schmalhofer, W. A., Borris, R., Goetz, M. A., Hensens, O. D., Bao, J.-M., Kayser, F., Parsons, W. H., Rupprecht, K., Garcia, M. L., Kaczorowski, G. J., and Slaughter, R. S. (1999) *Biochemistry 38*, 4922−4930.
14. Goetz, M. A., Hensens, O. D., Zink, D. L., Borris, R. P., Morales, F., Tamayo-Castillo, G., Slaughter, R. S., Felix, J., and Ball, R. G. (1998) *Tetrahedron Lett. 39*, 2895−2898.
15. Koo, G. C., Blake, J. T., Shah, K., Staruch, M. J., Dumont, F., Wunderler, D., Sanchez, M., McManus, O. B., Sirotina-Meisher, A., Fischer, P., Boltz, R. C., Goetz, M. A., Baker, R., Bao, J., Kayser, F., Rupprecht, K. M., Parsons, W. H., Tong, X.-C., Ita, I. E., Pivnichny, J., Vincent, S., Cunningham, P., Hora, D., Jr., Feeney, W., Kaczorowski, G., and Springer, M. S. (1999) *Cell. Immunol. 197*, 99−107.
16. Schmalhofer, W. A., Bao, J., McManus, O. B., Green, B., Matyskiela, M., Wunderler, D., Bugianesi, R. M., Felix, J. P., Hanner, M., Linde-Arias, A.-R., Ponte, C. G., Velasco, L., Koo, G., Staruch, M. J., Miao, S., Parsons, W. H., Rupprecht, K., Slaughter, R. S., Kaczorowski, G. J., and Garcia, M. L. (2002) *Biochemistry 41*, 7781−7784.
17. Hanner, M., Schmalhofer, W. A., Green, B., Bordallo, C., Liu, J., Slaughter, R. S., Kaczorowski, G. J., and Garcia, M. L. (1999) *J. Biol. Chem. 274*, 25237−25244.
18. Garcia-Calvo, M., Leonard, R. J., Novick, J., Stevens, S. P., Schmalhofer, W., Kaczorowski, G. J., and Garcia, M. L. (1993) *J. Biol. Chem. 268*, 18866−18874.
19. Ho, S. N., Hunt, H. D., Horton, R. M., Pullen, J. K., and Pease, L. R. (1989) *Gene 77*, 51−59.
20. Hanner, M., Vianna-Jorge, R., Kamassah, A., Schmalhofer, W. A., Knaus, H.-G., Kaczorowski, G. J., and Garcia, M. L. (1998) *J. Biol. Chem. 273*, 16289−16296.
21. Price, M., Lee, S. C., and Deutsch, C. (1989) *Proc. Natl. Acad. Sci. U.S.A. 86*, 10171−10175.
22. Kalman, K., Pennington, M. W., Lanigan, M. D., Nguyen, A., Rauer, H., Mahnir, V., Paschetto, K., Kem, W. R., Grissmer, S., Gutman, G. A., Christian, E. P., Cahalan, M. D., Norton, R. S., and Chandy, K. G. (1998) *J. Biol. Chem. 273*, 32697−32707.
23. Garcia, M. L., Hanner, M., and Kaczorowski, G. J. (1998) *Toxicon 36*, 1641−1650.
24. MacKinnon, R. (1991) *Nature 350*, 232−235.
25. Wunderler, D., Leonard, R. J., Sanchez, M., and McManus, O. B. (1999) *Biophys. J. 76*, A186.
26. Hanner, M., Green, B., Gao, Y.-D., Schmalhofer, W. A., Matyskiela, M., Durand, D. J., Felix, J. P., Linde, A.-R., Bordallo, C., Kaczorowski, G. J., Kohler, M., and Garcia, M. L. (2001) *Biochemistry 40*, 11687−11697.
27. Yellen, G., Sodickson, D., Chen, T.-Y., and Juman, M. E. (1994) *Biophys. J. 66*, 1068−1075.
28. Liu, Y., Jurman, M. E., and Yellen, G. (1996) *Neuron 16*, 859−867.
29. Willardsom, B. M., Pou, B., Yoshida, T., and Bitensky, M. W. (1993) *J. Biol. Chem.* 268, 6371−6382.

BI034122Q